Parametric characterization and estimation of bi-azimuth dispersion of path components

Yin, Xuefeng; Pedersen, Troels; Czink, Nicolai; Fleury, Bernard Henri

Published in:
The proceeding of the seventh IEEE International Workshop on Signal Processing Advances for Wireless Communications (SPAWC)

Publication date:
2006

Document Version
Publisher's PDF, also known as Version of record

Parametric Characterization and Estimation of Bi-Azimuth Dispersion of Path Components

Xuefeng Yin [1)], Troels Pedersen [1)], Nicolai Czink [3), 2)] and Bernard H. Fleury [1), 2)]

[1)] Information and Signals Division, Department of Communication Technology, Aalborg University, Aalborg, Denmark

[2)] Forschungszentrum Telekommunikation Wien (ftw.), Vienna, Austria

[3)] Institut für Nachrichtentechnik und Hochfrequenztechnik, Technische Universität Wien, Vienna, Austria

***Abstract*— In this contribution, we derive a probability distribution suitable for characterizing bi-azimuth (azimuth of arrival and azimuth of departure) direction dispersion of individual path components in the response of the propagation channel. This distribution belongs to the family of generalized von-Mises-Fisher distributions. The elements in this family maximize the entropy under the constraint that the expectations and correlation matrix of the directions are known. The probability density function (pdf) of the proposed distribution is used to describe the bi-azimuth power spectrum of individual path components. An estimator of the parameters of the pdf is derived and applied to characterize the spreads in both azimuth of departure and azimuth of arrival, as well as the correlation between both azimuths of individual path components. Preliminary results from an experimental investigation demonstrate the applicability of the proposed characterization in real environments.**

***Index Terms*— Path components, bi-azimuth dispersion, von-Mises-Fisher distribution, maximum-likelihood estimation.**

I. Introduction

Due to the heterogeneity of the propagation environment, the received signal at the receiver (Rx) of a radio communication system is the superposition of a number of components. Each individual component, which we call "path component", is contributed by an electromagnetic wave propagating along a path from the transmitter (Tx) to the Rx. Along this path, the wave interacts with a certain number of objects referred to as scatterers. Due to the geometrical and electromagnetic properties of the scatterers, the individual path components may be dispersive in delay, direction of departure (DoD), direction of arrival (DoA), polarizations, as well as in Doppler frequency when the environment is time-variant.

This work was jointly supported by the Network of Excellence in Wireless COMmunications (NEWCOM) and Elektrobit Testing Oy.

Path components can be observed in the response of the channel and any characterizing function derived from this response. As an example, in Fig. 1 we show two estimated power spectra with respect to azimuth of departure (AoD) and azimuth of arrival (AoA) at specific delays calculated from measurement data using the Bartlett beamformer [2]. In the sequel, we refer to these spectra as (bi-azimuth) Bartlett spectra. A certain number of spots can be observed. Each spot corresponds to either one or more specific path components. It can be observed from Fig. 1 (a) and (b) that the path components are spread in AoA and AoD. Moreover, they appear tilted. Both effects are due to the geometrical and electromagnetic properties of the scatterers along the paths, as well as the response – in particular the limited resolution – of the measurement equipment.

Recently, estimation of the characteristics of individual path components have gained much attention. The conventional approach consists in estimating the channel response and any characterizing functions derived from this response. An example of the characterizing function is the power spectrum and a traditional estimate of it

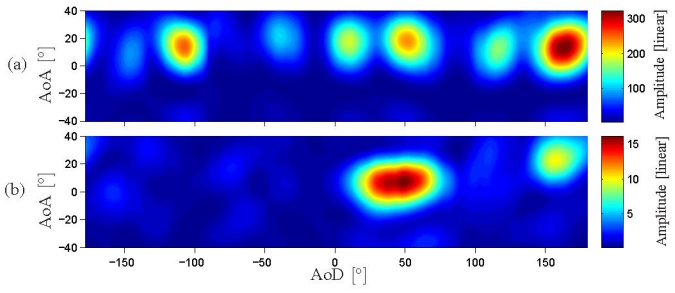

Fig. 1. Examples of two bi-azimuth Bartlett spectra calculated at specific relative delays (78 ns, 133 ns) from the correlator output of the channel sounder [1] in (a) an office; (b) a big hall. In the calculation, the responses of the Tx and Rx arrays in vertical-polarization only are considered. The details of the measurement campaign and measurement setup are provided in Section V.

is the Bartlett spectrum. However, due to the response of the measurement equipment, the path components are blurred and consequently, their spreads are artificially increased. In recent years, several model-based estimation techniques have been proposed to estimate the nominal azimuth and azimuth dispersion of the path components at one side of the link [3] [4] [5]. These techniques are based on the assumption that the azimuth power spectra of individual path components exhibit a shape which is close to that of the probability density function (pdf) of a certain distribution, like the uniform distribution [4], the (truncated) Gaussian distribution [3] [4] and the von-Mises distribution [5].

In this contribution, we propose an entropy-maximizing bi-direction (i.e. DoD and DoA) distribution to characterize bi-direction dispersion by means of the mean directions and correlation matrix between both directions. Such distributions have been derived in [6] and are called generalized von-Mises-Fisher distributions. We consider the case of horizontal-only propagation. The von-Mises-Fisher distribution is described by three free parameters (two vector parameters and one matrix parameter) that we identify. To do so, we assume that in the case where the path components are slightly dispersive the bi-azimuth distribution is close to a two-dimensional (2-D) truncated Gaussian distribution. Furthermore, we derive a maximum likelihood estimator for the parameters of the pdf of the von-Mises Fisher distribution. This estimator is applicable in time-variant environments, i.e. when fast-fading occurs [7].

The organization of this contribution is as follows. In Section II, we derive the pdf of the bi-variate von-Mises-Fisher distribution. Section III presents the signal model describing bi-azimuth dispersion of path components. The maximum likelihood estimator of the parameters of the pdf is derived in Section IV. Section V presents the result of the experimental investigation. Finally concluding remarks are made in Section VI.

II. Von-Mises-Fisher Distribution

Following the nomenclature in [8], we use a unit vector $\mathbf{\Omega}$ to characterize a direction. In the considered case of horizontal-only propagation, the vector $\mathbf{\Omega}$ has its initial point anchored at the origin O of a coordinate system specified in the region surrounding the array of interest, and terminal point located on a unit circle $\mathbb{S}_1$ centered at O. The vector $\mathbf{\Omega}$ is uniquely determined by its azimuth ϕ. The one-to-one relation between $\mathbf{\Omega}$ and ϕ is

$$\mathbf{\Omega} = \boldsymbol{e}(\phi) \doteq [\cos(\phi), \sin(\phi)]^{\mathrm{T}} \tag{1}$$

with $[\cdot]^{\mathrm{T}}$ denoting transposition.

Among all probability distributions on $\mathbb{S}_1$, the von-Mises distribution appears to be a natural candidate to describe direction dispersion by individual path components, provided the characterization of direction dispersion is only by means of the mean direction $\mathrm{E}[\mathbf{\Omega}]$[8]. The von-Mises distribution shares the same virtue as the Gaussian distribution, namely it maximizes the entropy among the family of probability distributions on the circle with the constraint that the second central moment is fixed. Notice that the second central moment of a circular distribution is the direction spread [8]. It is uniquely determined by the norm of the mean direction. Indeed, if $\sigma_{\mathbf{\Omega}}$ denotes the direction spread, then $\sigma_{\mathbf{\Omega}} = \sqrt{1 - \|\mathrm{E}[\mathbf{\Omega}]\|^2}$ [8]. The pdf of the von-Mises distribution reads [6, Sect. 2.1]

$$f(\mathbf{\Omega}) = \frac{1}{2\pi I_0(\kappa)} \exp\{\kappa \bar{\mathbf{\Omega}}^{\mathrm{T}} \mathbf{\Omega}\},$$

where $I_n(\cdot)$ is the modified Bessel function of the first kind and order n, $\kappa \geq 0$ is called the concentration parameter, and $\bar{\mathbf{\Omega}} \doteq \boldsymbol{e}(\bar{\phi})$ denotes a unit vector with azimuth $\bar{\phi}$ equal to the azimuth of $\mathrm{E}[\mathbf{\Omega}]$. The azimuth distribution induced by the von-Mises distribution via the mapping (1) has the pdf [9, P. 36]

$$f(\phi) = \frac{1}{2\pi I_0(\kappa)} \exp\{\kappa \cos(\phi - \bar{\phi})\}. \tag{2}$$

By a generalization of terminology, the azimuth probability distribution with the pdf (2) is referred to the von-Mises distribution as well.

Note that throughout the paper, azimuth variables are within the range $[-\pi, \pi)$. Addition and subtraction of azimuth variables are defined in such a way that the resulting angle lies in the range $[-\pi, \pi)$. When κ is large, typically $\kappa > 7$,

$$(\phi - \bar{\phi})^2 \;\approx\; \|\mathbf{\Omega} - \bar{\mathbf{\Omega}}\|^2 \tag{3}$$

holds, which leads to the approximation $\cos(\phi - \bar{\phi}) \approx 1 - \frac{1}{2}(\phi - \bar{\phi})^2$. Inserting this approximation in (2) yields the Gaussian pdf $f_{\mathrm{G}}(\phi) = \frac{\sqrt{\kappa}}{\sqrt{2\pi}} \exp\{-\frac{\kappa}{2}(\phi - \bar{\phi})^2\}$ [9, P. 37].

In the sequel, we derive a bivariate pdf of the DoA $\mathbf{\Omega}_1$ and the DoD $\mathbf{\Omega}_2$ for horizontal-only propagation. The symbols with subscript 1 and 2 are with respect to the Tx array and the Rx array respectively. It is shown in [6] that the maximum entropy bi-direction distribution when the expectations $\mathrm{E}[\mathbf{\Omega}_1]$ and $\mathrm{E}[\mathbf{\Omega}_2]$ and the correlation matrix $\mathrm{E}[\mathbf{\Omega}_1 \mathbf{\Omega}_2^{\mathrm{T}}]$ are specified has a pdf of the form

$$f(\mathbf{\Omega}_1, \mathbf{\Omega}_2) = C \cdot \exp\{\boldsymbol{a}_1^{\mathrm{T}} \mathbf{\Omega}_1 + \boldsymbol{a}_2^{\mathrm{T}} \mathbf{\Omega}_2 + \mathbf{\Omega}_1^{\mathrm{T}} \boldsymbol{A} \mathbf{\Omega}_2\}, \tag{4}$$

where C denotes a normalization factor, $\boldsymbol{a}_1, \boldsymbol{a}_2 \in \mathbb{R}^{2\times 1}$ and $\boldsymbol{A} \in \mathbb{R}^{2\times 2}$. Following [6] we refer to this distribution as the generalized von-Mises-Fisher distribution.

The parameters $\boldsymbol{a}_1$, $\boldsymbol{a}_2$ and $\boldsymbol{A}$ in (4) are free parameters, the specification of which depends on the particular problem at hand. To find the appropriate expressions of $\boldsymbol{a}_1$, $\boldsymbol{a}_2$ and $\boldsymbol{A}$ for our particular application, i.e. the characterization of bi-azimuth dispersion, we postulate that, for slightly distributed path components, the bi-azimuth pdf induced by (4) via the mapping (1) should be close to the truncated pdf of a 2-D Gaussian distribution:

$$f_{\mathrm{G}}(\phi_1,\phi_2) \;\propto\; \exp\Bigg\{-\frac{1}{2(1-\rho^2)}\cdot \left[\left(\frac{\phi_1-\bar{\phi}_1}{\sigma_1}\right)^2+\left(\frac{\phi_2-\bar{\phi}_2}{\sigma_2}\right)^2-\frac{2\rho(\phi_1-\bar{\phi}_1)(\phi_2-\bar{\phi}_2)}{\sigma_1\sigma_2}\right]\Bigg\}. \quad (5)$$

Notice that the traditional meaning of the parameters σ_1, σ_2 and ρ as second-order central moments of a bivariate Gaussian distribution does not hold any more for the pdf (5) due to the fact that the azimuth ranges are bounded.

In the case where the path components are slightly dispersive, the approximation in (3) is valid for both AoA and AoD. In addition, the approximation

$$(\phi_1-\bar{\phi}_1)(\phi_2-\bar{\phi}_2) \;\approx\; (\boldsymbol{\Omega}_1-\bar{\boldsymbol{\Omega}}_1)^{\mathrm{T}}\boldsymbol{R}(\boldsymbol{\Omega}_2-\bar{\boldsymbol{\Omega}}_2) \quad (6)$$

holds where

$$\boldsymbol{R} \doteq \boldsymbol{B}(\bar{\phi}_1)\boldsymbol{B}(\bar{\phi}_2)^{\mathrm{T}} = \begin{bmatrix}\cos(\bar{\phi}_1-\bar{\phi}_2) & -\sin(\bar{\phi}_1-\bar{\phi}_2)\\ \sin(\bar{\phi}_1-\bar{\phi}_2) & \cos(\bar{\phi}_1-\bar{\phi}_2)\end{bmatrix}.$$

The matrix $\boldsymbol{B}(\bar{\phi})$ is the orthonormal matrix that rotates the vector $\boldsymbol{e}(\bar{\phi})$ to $[0,1]^{\mathrm{T}}$. Hence, $\boldsymbol{B}(\bar{\phi}) \doteq [\boldsymbol{e}^{\perp}(\bar{\phi})\;\; \boldsymbol{e}(\bar{\phi})]$ with $\boldsymbol{e}^{\perp}(\bar{\phi}) = \boldsymbol{e}(\bar{\phi}+\pi/2)$ denoting the unit vector portside orthogonal to $\boldsymbol{e}(\bar{\phi})$. The right-hand-side of (6) is rotational invariant, i.e. it does not change when for any specific index $i \in \{1,2\}$, $\boldsymbol{\Omega}_i$, $\bar{\boldsymbol{\Omega}}_i$ and $\boldsymbol{e}(\bar{\phi}_i)$ are rotated by an identical arbitrary azimuth.

Inserting (3) and (6) into (5) and identifying (4) and (5), we obtain after some straightforward algebraic manipulations

$$\boldsymbol{a}_i \approx \frac{\kappa_i}{1-\rho^2}\Big(1-\rho\sqrt{\frac{\kappa_j}{\kappa_i}}\Big)\bar{\boldsymbol{\Omega}}_i, \quad i,j\in\{1,2\},\; i\neq j$$

$$\boldsymbol{A} \approx \frac{\rho\sqrt{\kappa_1\kappa_2}}{1-\rho^2}\boldsymbol{R}$$

with the definitions $\kappa_i \doteq \sigma_i^{-2}$, $i=1,2$. Inserting the right-hand-sides in (4) yields the sought pdf:

$$f(\boldsymbol{\Omega}_1,\boldsymbol{\Omega}_2) \;=\; C\cdot\exp\Bigg\{\frac{\kappa_1-\rho\sqrt{\kappa_1\kappa_2}}{1-\rho^2}\bar{\boldsymbol{\Omega}}_1^{\mathrm{T}}\boldsymbol{\Omega}_1+ \frac{\kappa_2-\rho\sqrt{\kappa_1\kappa_2}}{1-\rho^2}\bar{\boldsymbol{\Omega}}_2^{\mathrm{T}}\boldsymbol{\Omega}_2+\frac{\rho\sqrt{\kappa_1\kappa_2}}{1-\rho^2}\boldsymbol{\Omega}_1^{\mathrm{T}}\boldsymbol{R}\boldsymbol{\Omega}_2\Bigg\}. \quad (7)$$

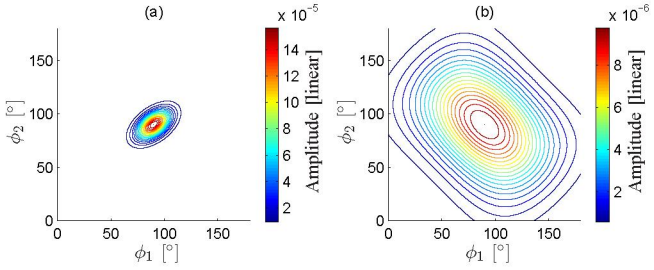

Fig. 2. Contour plots of the bi-azimuth pdf (8) with parameter settings $\bar{\phi}_1 = \bar{\phi}_2 = 90°$ and (a) $(\kappa_1,\kappa_2,\rho) = (30,40,0.5)$, (b) $(\kappa_1,\kappa_2,\rho) = (2,2,-0.5)$.

The normalization constant C can be computed from the expression derived in [10, P. 167] for the general form (7):

$$C \;=\; \Bigg[4\pi^2\sum_{m=0}^{\infty} m\cdot I_m\left(\frac{\kappa_1-\rho\sqrt{\kappa_1\kappa_2}}{1-\rho^2}\right) \cdot I_m\left(\frac{\rho\sqrt{\kappa_1\kappa_2}}{1-\rho^2}\right) I_m\left(\frac{\kappa_2-\rho\sqrt{\kappa_1\kappa_2}}{1-\rho^2}\right)\Bigg]^{-1}.$$

From (7) the joint pdf of ϕ_1 and ϕ_2 is calculated to be

$$f(\phi_1,\phi_2) \;=\; C\cdot\exp\Bigg\{\left(\frac{\kappa_1-\rho\sqrt{\kappa_1\kappa_2}}{1-\rho^2}\right)\cos(\phi_1-\bar{\phi}_1) + \left(\frac{\kappa_2-\rho\sqrt{\kappa_1\kappa_2}}{1-\rho^2}\right)\cos(\phi_2-\bar{\phi}_2) + \frac{\rho\sqrt{\kappa_1\kappa_2}}{1-\rho^2}\cos[(\phi_1-\bar{\phi}_1)-(\phi_2-\bar{\phi}_2)]\Bigg\}. \quad (8)$$

Fig. 2 illustrates the contour plots of (8) for two different settings of the parameters κ_1, κ_2 and ρ. It can be observed that when κ_1 and κ_2 are large, the contour lines are close to tilted ellipses. This is consistent with the fact that the pdf (8) is close to a bivariate normal pdf in this case. When both κ_1 and κ_2 are small, the contour lines are still close to ellipses in a range enclosing $(\bar{\phi}_1,\bar{\phi}_2)$. This observation indicates that in this region the pdf (8) can be approximated by a bivariate normal pdf as well.

III. Signal Model for Bi-azimuth Dispersion by Path Components in MIMO Channel Sounding

We consider horizontal-only propagation and narrowband transmission. The latter condition implies that the product of the signal bandwidth times the channel delay spread is much smaller than one. Following the nomenclature in [8], the continuous-time output signal

of the Rx array reads

$$\begin{aligned}\boldsymbol{Y}(t) &= \boldsymbol{H}(t)\boldsymbol{s}(t) + \boldsymbol{W}(t) \\ &= \left[\iint \boldsymbol{c}_2(\phi_2)\boldsymbol{c}_1(\phi_1)^{\mathrm{T}} h(t;\phi_1,\phi_2)\mathrm{d}\phi_1\mathrm{d}\phi_2\right]\boldsymbol{s}(t) \\ &\quad + \boldsymbol{W}(t). \end{aligned} \tag{9}$$

The M_2-D complex vector $\boldsymbol{Y}(t) \in \mathbb{C}^{M_2\times 1}$ contains the output signals of the Rx array observed at time instance t. The matrix $\boldsymbol{H}(t) \in \mathbb{C}^{M_2\times M_1}$ represents the time-variant transfer matrix of the MIMO system. The M_1-D vector $\boldsymbol{s}(t) \in \mathbb{C}^{M_1\times 1}$ denotes the complex envelope of the transmitted signal. The function $h(t;\phi_1,\phi_2)$ is referred to as the (time-variant) bi-azimuth spread function of the propagation channel [8]. In a scenario where the electromagnetic energy propagates from the Tx to the Rx via D paths, $h(t;\phi_1,\phi_2)$ can be decomposed as

$$h(t;\phi_1,\phi_2) = \sum_{d=1}^{D} h_d(t;\phi_1,\phi_2). \tag{10}$$

The summand $h_d(t;\phi_1,\phi_2)$ denotes the dth path component in $h(t;\phi_1,\phi_2)$. The noise component $\boldsymbol{W}(t) \in \mathbb{C}^{M_2\times 1}$ in (9) is a vector-valued circularly symmetric, spatially and temporally white Gaussian process with component spectral height σ_w^2. Finally, the complex vectors $\boldsymbol{c}_i(\phi) \doteq [c_{i,1}(\phi),\ldots,c_{i,m_i}(\phi),\ldots,c_{i,M_i}(\phi)]^{\mathrm{T}} \in \mathbb{C}^{M_i\times 1}$, $i = 1, 2$ are the responses of the Tx array ($i = 1$) and the Rx array ($i = 2$).

Moreover, we make the following assumptions regarding the properties of some components in (9):

a) The channel is sounded during N non-overlapping intervals of duration T. Thus, the overall sounding period is of the form $\bigcup_{n=1}^{N}[t_n, t_n + T)$ where t_n denotes the beginning of the nth interval and $t_{n+1} > t_n + T$, $n = 1,\ldots,N$.

b) The sounding signal $\boldsymbol{s}(t)$ is known to the Rx. Its components are orthonormal[1], i.e. $\int_{t_n}^{t_n+T} \boldsymbol{s}(t)\boldsymbol{s}(t)^{\mathrm{H}}\mathrm{d}t = \boldsymbol{I}_{M_1}$, $n \in [1,\ldots,N]$. Here, $\boldsymbol{I}_{(\cdot)}$ denotes an identity matrix of dimension given as an index.

c) The transfer matrix $\boldsymbol{H}(t)$ fluctuates over the overall sounding period, but it is constant within individual observation intervals: $\boldsymbol{H}(t) = \boldsymbol{H}(t_n) \doteq \boldsymbol{H}_n$, $t \in [t_n, t_n + T)$. Similarly, the bi-azimuth spread function $h_d(t;\phi_1,\phi_2)$ arising in (10) is constant within individual observation intervals: $h_d(t;\phi_1,\phi_2) = h_d(t_n;\phi_1,\phi_2) \doteq h_{d,n}(\phi_1,\phi_2)$, $t \in [t_n, t_n + T)$. The processes $h_{d,n}(\phi_1,\phi_2)$, $n \in [1,\ldots,N]$, $d \in [1,\ldots,D]$ are uncorrelated complex (zero-mean) orthogonal stochastic measures, i.e.

$$\begin{aligned}&\mathrm{E}[h_{d,n}^*(\phi_1,\phi_2)h_{d',n'}(\phi_1',\phi_2')] = \\ &\quad P_d(\phi_1,\phi_2)\delta_{nn'}\delta_{dd'}\delta(\phi_1-\phi_1')\delta(\phi_2-\phi_2'),\end{aligned} \tag{11}$$

where $(\cdot)^*$ denotes the complex conjugate, $\delta_{(\cdot)}$ and $\delta(\cdot)$ represent the Kronecker delta and the Dirac delta function respectively, and $P_d(\phi_1,\phi_2) \doteq \mathrm{E}[|h_{d,n}(\phi_1,\phi_2)|^2]$ is the bi-azimuth power spectrum of the dth path component. Thus, identity (11) implies that the spread functions of different individual path components or at different observation intervals are uncorrelated. This scenario is referred to as the *incoherent-distributed-source* case in the literature (see e.g. [12]).

d) The spectrum $P_d(\phi_1,\phi_2)$ describes the manner the average power of the dth path component is distributed with respect to both AoD and AoA. We assume $P_d(\phi_1,\phi_2) = P_d \cdot f_d(\phi_1,\phi_2)$ with P_d representing the total average power of the dth path component and $f_d(\phi_1,\phi_2)$ being of the form (8) with path-specific parameters

$$\boldsymbol{\theta}_d \doteq [\bar{\phi}_{d,1}, \bar{\phi}_{d,2}, \kappa_{d,1}, \kappa_{d,2}, \rho_d].$$

[1]The orthogonality of the signal components can be obtained by using different sounding techniques, such as time-division [11] and frequency-division multiplexing. It can be also nearly achieved by using different pseudo-noise (PN) sequences or differently-shifted versions of the same PN sequence as the components of the sounding signal $\boldsymbol{s}(t)$.

IV. Maximum Likelihood Estimation

Let $\boldsymbol{\theta}$ denote a vector containing the model parameters in (9)

$$\boldsymbol{\theta} \doteq [\sigma_w^2, P_1, P_2, \ldots, P_D, \boldsymbol{\theta}_1, \boldsymbol{\theta}_2, \ldots, \boldsymbol{\theta}_D].$$

Under the assumption that the components of $\boldsymbol{s}(t)$ are orthonormal, the $M_2 \times M_1$ matrices

$$\widehat{\boldsymbol{H}}_n \doteq \int_{t_n}^{t_n+T} \boldsymbol{y}(t)\boldsymbol{s}(t)^{\mathrm{H}}\mathrm{d}t, \quad n = 1,\ldots,N \tag{12}$$

form a sufficient statistic for the estimation of $\boldsymbol{\theta}$. It can be shown that $\widehat{\boldsymbol{H}}_n = \boldsymbol{H} + \boldsymbol{N}_n$ where $\boldsymbol{N}_n \in \mathbb{C}^{M_2\times M_1}$, $n = 1,\ldots,N$ is a sequence of independent random matrices the entries of which are independent circularly symmetric Gaussian random variables with variance σ_w^2.

The maximum likelihood estimate of $\boldsymbol{\theta}$ based on the observation $\boldsymbol{Y}(t) = \boldsymbol{y}(t)$ during the sounding interval $\bigcup_{n=1}^{N}[t_n, t_n + T)$ is a solution of [2]:

$$\hat{\boldsymbol{\theta}} \doteq \arg\max_{\boldsymbol{\theta}}\{-\ln[|\boldsymbol{\Sigma}|] - \mathrm{tr}\big[(\boldsymbol{\Sigma})^{-1}\hat{\boldsymbol{\Sigma}}\big]\} \tag{13}$$

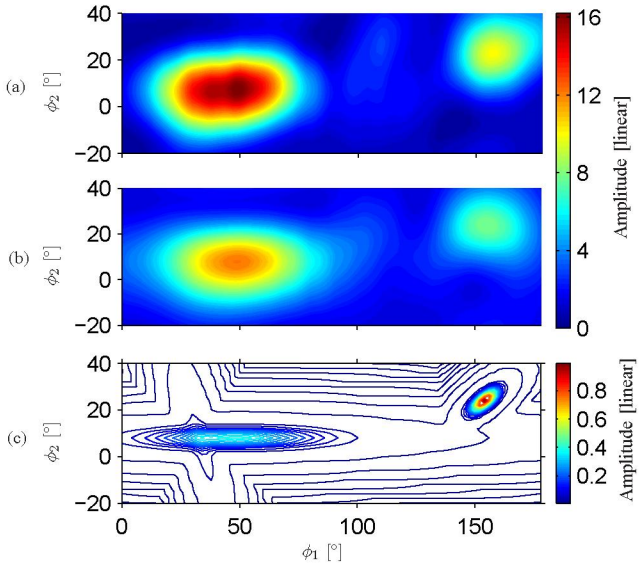

Fig. 3. (a): Bi-azimuth Bartlett spectrum calculated from the received signal as is; (b): Bi-azimuth Bartlett spectrum calculated from the matrix $\boldsymbol{\Sigma}$ in (14) parameterized with the estimate $\hat{\boldsymbol{\theta}}$; (c): Contour lines of the estimated bi-azimuth power spectrum using the proposed characterization by means of the von-Mises-Fisher pdf (8).

with $\mathrm{tr}[\cdot]$ representing the trace of the matrix given as an argument and

$$\begin{aligned}\boldsymbol{\Sigma} &\doteq \mathrm{E}\big[\mathrm{vec}[\widehat{\boldsymbol{H}}_n]\cdot\mathrm{vec}[\widehat{\boldsymbol{H}}_n]^{\mathrm{H}}\big] \\ &= \sum_{d=1}^{D} P_d \iint [\boldsymbol{c}_1(\phi_1)\boldsymbol{c}_1^{\mathrm{H}}(\phi_1)]\otimes[\boldsymbol{c}_2(\phi_2)\boldsymbol{c}_2^{\mathrm{H}}(\phi_2)] \\ &\quad \cdot f_d(\phi_1,\phi_2)\mathrm{d}\phi_1\mathrm{d}\phi_2 + \sigma_w^2\boldsymbol{I}_{M_2M_1}, \end{aligned} \tag{14}$$

where the operator $\mathrm{vec}[\cdot]$ stacks the columns of the given matrix into a vector and $\otimes$ denotes the Kronecker product. In (13) the matrix $\hat{\boldsymbol{\Sigma}} = \frac{1}{N}\sum_{n=1}^{N}\mathrm{vec}[\widehat{\boldsymbol{H}}_n]\mathrm{vec}[\widehat{\boldsymbol{H}}_n]^{\mathrm{H}}$ is an estimate of $\boldsymbol{\Sigma}$ computed from the observation $\boldsymbol{y}(t)$ over $\bigcup_{n=1}^{N}[t_n, t_n+T)$.

Calculation of $\hat{\boldsymbol{\theta}}$ requires $(5D+1)$-D maximization operations. The SAGE algorithm described in [13] can be used to compute a low-complexity approximation of the maximum likelihood estimator in (13).

V. Preliminary Experimental Investigation

In this section, we assess the applicability of the characterization by means of the von-Mises-Fisher pdf (8) in a real environment. The measurement data were obtained with the MIMO wideband radio channel sounder Elektrobit Propsound CS [1]. The measurement campaign was conducted in a big hall at a center frequency of 5.2 GHz with bandwidth 100 MHz. The Tx and Rx were both equipped with two similar 9-element circular arrays. The polarization direction of the elements is 45° slanted with respect to the vertical. The positions of the Rx and Tx were kept fixed. The hall was crowded with people moving around during the measurement runs. This introduced time variations of the channel response. The equipment collects wideband measurement data. However, the narrowband model developed in Sect. III can still be applied by considering the correlator output of the channel sounder at some specific relative delay.

TABLE I

Parameter estimates in the experimental investigation.

d	$\hat{\bar{\phi}}_{d,1}$	$\hat{\bar{\phi}}_{d,2}$	$\hat{\kappa}_{d,1}$	$\hat{\sigma}_{d,1}$	$\hat{\kappa}_{d,2}$	$\hat{\sigma}_{d,2}$	$\hat{\rho}_d$	$\hat{P}_d/\widehat{\sigma_w^2}$
1	48°	8°	6.29	22.9°	480	2.6°	0.02	15.5 dB
2	34°	4°	153.75	4.6°	18.36	13.4°	−0.83	4.69 dB
3	154°	24°	233.02	3.8°	320	3.2°	0.70	11.1 dB

We specifically selected a propagation scenario and for that scenario, a relative delay at which only few path components can be observed. The Bartlett spectrum shown in Fig. 1 (b) corresponds to such a situation with two or, possibly, three path components. Portion of this Bartlett spectrum including the path components is reproduced in Fig. 3 (a).

The SAGE algorithm is used to estimate the parameters of the path components. In this preliminary study, we assume that the number of path components is known in advance. In the considered case, this number equals 3, which coincides with the amount of the path components that can be visually identified from the Bartlett spectrum shown in Fig. 1 (b). We consider vertical polarization only, i.e. the vectors $\boldsymbol{c}_i(\phi)$, $i=1,2$ used in the calculation of $\boldsymbol{\Sigma}$ in (14) are the array responses for vertical polarization. The initial estimates of the parameters of the individual path components are computed using a combination of the successive interference cancelation method described in [13] and an estimator derived based on the generalized array manifold model [14]. At each iteration of the SAGE algorithm, the parameter estimates of one path component and the estimate of the noise spectral height σ_w^2 are updated. The admissible hidden data is selected to be the sum of the path component, of which the parameters are estimated, and an M_2-D noise vector with statistical properties identical to those of $\boldsymbol{W}(t)$ weighted by $1/\sqrt{3}$. The definition and meaning of the weighting factor are given in [13].

The obtained parameter estimates are reported in Table I. Estimates $\hat{\sigma}_{d,i} = \sqrt{1/\hat{\kappa}_{d,i}}$, $d=1,2,3$, $i=1,2$ of the azimuth spreads of the path components expressed in degree are also provided. Fig. 3 (c) depicts the estimated bi-azimuth power spectrum

$$\hat{P}(\phi_1,\phi_2) = \sum_{d=1}^{3}\hat{P}_d\hat{f}_d(\phi_1,\phi_2), \tag{15}$$

where $\hat{f}_d(\phi_1, \phi_2)$ denotes the pdf $f(\phi_1, \phi_2)$ in (8) parameterized with the estimate $\hat{\boldsymbol{\theta}}_d$. From Fig. 3 (c), we observe that the path components are significantly more concentrated than the corresponding components in the Bartlett spectrum shown in Fig. 3 (a). Moreover, the third path component in Fig. 3 (c) appears to be stronger than the first component even though $\hat{P}_3 < \hat{P}_1$. This is because the power spectrum of the third path component is more concentrated than the spectrum of the first component.

Fig. 3 (b) depicts the Bartlett spectrum calculated from the reconstructed signal with the bi-azimuth power spectrum (15). Notice that the spectral height estimate $\widehat{\sigma_w^2}$ is also considered in the calculation. The blurring effect due to the limited resolution in azimuth of the used arrays is clearly demonstrated. As a result, the path components in the Bartlett spectrum exhibit significantly larger spreads compared to the spreads of the estimated components. Notice that the Bartlett spectrum shown in Fig. 3 (b) looks similar to the spectrum in Fig. 3 (a). Furthermore, it is observed that the magnitude of the path components depicted in Fig. 3 (b) is lower than that observed in Fig. 3 (a). This is consistent with an analytical result not reported here, which shows that the power estimate of a path component is reduced, compared to the true value, by a certain amount depending on the residual interference. This interference results since the path components are not estimated exactly due to either model mismatch or errors in the parameter estimation.

Calculations show that the ratio of the maximum of the Bartlett spectrum computed from the reconstructed signal with $\widehat{\sigma_w^2} = 0$ to the maximum of the Bartlett spectrum calculated from the received signal, is equal to 68.7%. Experimental investigations also show that this number reduces to 37.7% when the ISIS algorithm [11] derived based on the specular-scatterer model is applied to the same measurement data. This observation, together with the conclusions drawn from Fig. 3, demonstrate that the von-Mises-Fisher pdf (8) provides an appropriate characterization of bi-azimuth dispersion by individual path components.

VI. Conclusions

In this contribution, we proposed a bi-variate generalized von-Mises-Fisher probability density function (pdf) suitable for characterizing bi-azimuth (azimuth of arrival and azimuth of departure) dispersion of individual path components. We also derived an estimator of the parameters of the pdf. Preliminary experimental results demonstrated the applicability of the proposed characterizing method in real situations. These results also made evident that the path components are noticeably more concentrated in the bi-azimuth plane compared to their corresponding footprints in the Bartlett spectrum.

References

[1] E. Bonek, N. Czink, V. Holappa, M. Alatossava, L. Hentilä, J. Nuutinen, and A. Pal, "Indoor MIMO measurements at 2.55 and 5.25 GHz - a comparison of temporal and angular characteristics," 2006, submitted to IST Mobile Summit 2006.

[2] H. Krim and M. Viberg, "Two decades of array signal processing research: the parametric approach," *IEEE Trans. Signal Processing*, vol. 13, pp. 67–94, 1996.

[3] T. Trump and B. Ottersten, "Estimation of nominal direction of arrival and angular spread using an array of sensors," *Signal Processing*, pp. 50(1–2):57–69, Apr. 1996.

[4] O. Besson and P. Stoica, "Decoupled estimation of DoA and angular spread for spatially distributed sources," *IEEE Trans. Signal Processing*, vol. 49, pp. 1872–1882, 1999.

[5] C. Ribeiro, E. Ollila, and V. Koivunen, "Stochastic maximum likelihood method for propagation parameter estimation," in *15th IEEE International Symposium on Personal, Indoor and Mobile Radio Communications, 2004. PIMRC 2004.*, vol. 3, Sept. 5-8 2004.

[6] K. V. Mardia, "Statistics of directional data," *Journal of the Royal Statistical Society. Series B (Methodological)*, vol. 37, pp. 349–393, 1975.

[7] M. Bengtsson and B. Ottersten, "Low-complexity estimators for distributed sources," *IEEE Trans. Signal Processing*, vol. 48, no. 8, pp. 2185–2194, Aug. 2000.

[8] B. H. Fleury, "First- and second-order characterization of direction dispersion and space selectivity in the radio channel," *IEEE Trans. Information Theory*, no. 6, pp. 2027–2044, Sept. 2000.

[9] K. V. Mardia and P. E. Jupp, *Directional Statistics*. John Wiley and Sons, Ltd., 2000.

[10] P. E. Jupp and K. V. Mardia, "A general correlation coefficient for directional data and related regression problems," *Biometrika*, vol. 67, pp. 163–173, 1980.

[11] B. H. Fleury, P. Jourdan, and A. Stucki, "High-resolution channel parameter estimation for MIMO applications using the SAGE algorithm," in *2002 Int. Zurich Seminar on Broadband Communications (IZS 2002)*, 2002.

[12] S. Shahbazpanahi, S. Valaee, and M. Bastani, "Distributed source localization using ESPRIT algorithm," *Signal Processing, IEEE Transactions on*, vol. 49, Issue 10, pp. 2169–2178, 2001.

[13] B. H. Fleury, M. Tschudin, R. Heddergott, D. Dahlhaus, and K. L. Pedersen, "Channel parameter estimation in mobile radio environments using the SAGE algorithm," *IEEE Journal on Selected Areas in Communications*, vol. 17, no. 3, pp. 434–450, Mar. 1999.

[14] D. Asztély, B. Ottersten, and A. L. Swindlehurst, "A generalized array manifold model for local scattering in wireless communications," *Proc. IEEE Int. Conf. Acoust., Speech, Signal Processing, ICASSP '97*, 1997.